

Original Manuscript

Functional analysis of novel *RUNX2* mutations in cleidocranial dysplasia

Li Zeng¹, Jiahui Wei¹, Dong Han¹, Haochen Liu¹, Yang Liu¹, Na Zhao¹, Shichen Sun¹, Yixiang Wang^{2,*} and Hailan Feng¹

¹Department of Prosthodontics, Peking University School and Hospital of Stomatology, Beijing, PR China and ²Central Laboratory, Peking University School and Hospital of Stomatology, Beijing, PR China

*To whom correspondence should be addressed. 22 Zhongguancun Avenue South, Haidian District, Beijing 100081, China. Email: kqwangyx@bjmu.edu.cn

Received 23 February 2017; Revised 28 March 2017; Editorial decision 30 March 2017; Accepted 7 April 2017.

Abstract

Cleidocranial dysplasia (CCD) is a rare autosomal dominant skeletal disorder caused by mutation of runt-related transcription factor 2 (*RUNX2*) gene. The purpose of this study was to explore novel *RUNX2* mutations in seven individuals with CCD and investigate the function of the mutant *RUNX2* proteins. DNA samples were prepared from the peripheral blood of the CCD individuals, and then subjected to DNA sequencing. Conservation and secondary structure analysis were performed based on *RUNX2* sequencing results. pEGFP-C1 plasmids containing GFP-tagged wild-type *RUNX2* and three novel *RUNX2* mutations expression cassettes were constructed, and then transfected into HEK293T cells. Cell fluorescence, luciferase assay and western blotting were used to analyse the subcellular distribution and function of the mutant *RUNX2* proteins. Three novel mutations (R193G, 258fs, Y400X) were found in the seven CCD patients. Conservation and structure analysis show one novel mutation (R193G) in Runt domain and two novel mutations (258fs and Y400X) in PST domain of *RUNX2*. Western blotting confirmed that the 258fs and Y400X mutations produced truncated proteins. Fluorescence detection showed that the three novel mutants localised exclusively in the nucleus. However, luciferase assay indicated all mutants severely impaired the transactivation activities of *RUNX2* on osteocalcin promoter. Our results broaden the spectrum of *RUNX2* mutations in CCD individuals and demonstrated that loss of function in *RUNX2* is responsible for CCD.

Introduction

Cleidocranial dysplasia (CCD; OMIM # 119600) is a rare autosomal dominant skeletal disorder and the primary clinical features of CCD are mainly manifested in the bone and teeth. The main clinical features of bone include persistently open or delayed closure of fontanelles, brachycephalic skull, Wormian bones, hypoplastic and/or aplastic clavicles, wide pubic symphysis, distal phalanx dysplasia, short stature and other skeletal abnormalities; the phenotype of teeth including supernumerary teeth, delayed eruption of permanent teeth, retention of deciduous teeth, malocclusion and teeth hypoplasia (1–3). Although the phenotype of CCD is mainly manifested in the bone and teeth, these abnormalities are not observed in all individuals. The phenotypic spectrum differs dramatically, from slightly affected individuals with only supernumerary teeth to severely

affected individuals with the above typical CCD features (1). Interestingly, although numerous skeletal deficiencies are observed in CCD individuals, the dental abnormalities are usually the main complaints of the CCD individuals, owing to problems significantly affecting their pronunciation, speech and beauty.

Previous studies have demonstrated that mutation of the runt-related transcription factor 2 (*RUNX2*) gene is responsible for CCD (4,5). *RUNX2* is a member of *RUNX* family located on chromosome 6p21 and essential for osteoblast differentiation and skeletal morphogenesis (6,7). As the master transcriptional factor involved in bone formation, *RUNX2* regulates the expression of many bone matrix genes that characterise the osteoblasts and chondrocytes, including osteocalcin, bone sialoprotein, osteopontin and collagen I (8–10). Bone development needs a precise spatio-temporal regulation of *RUNX2* expression and a variety of factors have been

involved in this process. For example, Twist, Msh homeobox 2 (Msx2), and promyelocytic leukemia zinc-finger protein (PLZF) are acting upstream of *RUNX2*, Osterix (Osx) is acting downstream of *RUNX2* (11). Homozygous (*RUNX2*^{-/-}) mice died shortly after birth and failed in bone formation (12); while heterozygous (*RUNX2*^{+/-}) mice manifested similar to the CCD individuals, with morphological defects in the skeletal system but no teeth problems (13,14).

The *RUNX2* gene contains 8 exons and comprises a region of 130 kb in size, and has two potential translation start sites which can encode two major isoforms (15). The *RUNX2* protein contains 521 amino acids and several functional domains have been described. The first 19 amino acids are named the first activation domain (AD1). QA domain contains glutamine–alanine repeats with a transactivation activity (1). The Runt homologous domain (RHD) is a highly conserved motif that contains 128 amino acids and is responsible for DNA binding and protein heterodimerisation with the help of core-binding factor subunit beta (CBFβ). The RHD domain is closely followed by a nine amino acid sequence (PRRHRQKLD), which can serve as nuclear localisation signal (NLS); this domain is also highly conserved and essential for the accumulation of *RUNX2* protein in the nucleus (1). Towards the C-terminus is a proline–serine–threonine-rich region (PST) vital for transcriptional activity (1). In the PST region, there is a nuclear matrix targeting sequence (NMTS), which can affect *RUNX2* subnuclear localisation and serve as binding affinity to other proteins (16). At the end of the C-terminus, there is a 5 amino acid sequence named the VWRPY pentapeptide sequence; this motif is also highly conserved and involved in functional interactions with transcriptional co-repressors (1).

Though numerous mutations in *RUNX2* have been identified in CCD individuals, including nonsense, insertions, deletions, missense mutations and triplet expansion in the alanine-stretch (1,17,18), the mutation spectrum is still growing. Therefore, identification of *RUNX2* mutation in CCD individuals is meaningful for amplifying the spectrum of mutations and the functional researches of *RUNX2* mutants. In this study, we analysed the coding sequence of the *RUNX2* gene in seven individuals with the clinical diagnosis of CCD. The purpose of this study was to determine the genetic background of those individuals and to explore the function of those *RUNX2* mutants.

Materials and methods

CCD individuals recruitment

This study was approved by the Ethics Committee of Peking University School and Hospital of Stomatology. All individuals participated in this study with informed consent. Seven individuals from four unrelated families with clinical diagnosis of CCD were collected in this study.

Mutation detection

DNA samples were prepared from the peripheral blood of the CCD individuals by Universal Genomic DNA Kit (Cwbiochem, Beijing, China) according to the manufacturer's protocol. All of the exons of *RUNX2* gene were amplified by polymerase chain reaction (PCR) with the primers as described previously (1). PCR reactions were performed in a total volume of 50 µl, containing 25 µl Taq PCR master mix (Biomed, Beijing, China), 2 µl DNA, 2 µl primer pair and 21 µl ddH₂O. In a thermal cycler (Eppendorf, Hamburg, Germany), amplification was performed by an initial denaturation at 95°C for 5 min, followed by 40 cycles of 94°C for 20 s, 60°C for 30 s and 72°C for 1 min, finally followed with a 7-min extension at 72°C. The amplification products were examined by 2% agarose gel electrophoresis and purified with the Gel Extraction Kit (Cwbiochem). Sequencing process was performed on an ABI 3730 XL sequencer (ABI, Foster City, CA, USA).

Sequence results were analysed using the whole database of NCBI. We confirmed every mutation by at least two independent PCRs of the genomic DNA products and two independent sequencings.

Conservation and secondary structural analysis

Conservation analysis was conducted by Cluster X. Secondary structure of wild-type and mutants *RUNX2* were predicted by PsiPred 3.3 (<http://bioinf.cs.ucl.ac.uk/psipred>).

Plasmid preparation

The full length of wild-type *RUNX2* cDNA was subcloned into pEGFP-C1 (Mock) vector with Bgl II and Sal I and named as pEGFP-C1-*RUNX2* (WT). *In vitro* site-directed mutagenesis was performed for the construction of pEGFP-C1-R193G (R193G), pEGFP-C1-258fs (258fs) and pEGFP-C1-Y400X (Y400X) with the use of the QuikChange lightning site-directed mutagenesis kit (Stratagene, La Jolla, CA, USA). The entire coding sequence of wild-type and mutant *RUNX2* plasmid were confirmed. All the plasmids were constructed by Hanheng Chem Technology (Hanheng Chem, Shanghai, China). The *RUNX2*-responsive osteocalcin promoter linked to the luciferase gene (p6OSE2-luc) reporter plasmid and the pRL-TK renilla luciferase vector were a generous gift from Dr. X.L. Zhang (Department of Pediatric Dentistry, Peking University School and Hospital of Stomatology).

Cell culture and transfection

Human embryonic kidney (HEK) 293T cells were cultured in Dulbecco's Modified Eagle Medium (DMEM, Gibco, Paisley, UK) supplemented with 10% fetal bovine serum (Gibco), and 1% penicillin–streptomycin (Gibco). Cells were cultured in humidified atmosphere with 5% CO₂ and 95% air at 37°C. The medium was changed for every 2 days. Transient transfection was conducted with Lipofectamine 3000 (Invitrogen, Carlsbad, CA, USA) according to the manufacturer's instructions. At the indicated time, cells were analysed by western blotting or cell fluorescence.

Western blotting

At 48-h post-transfection, cells were collected and lysed in RIPA buffer with protease inhibitors. Western blotting was performed with cell lysates containing 30 µg of proteins. After sodium dodecyl sulfate polyacrylamide gel electrophoresis, the proteins were transferred to polyvinylidene difluoride membrane, which was blocked in 6% skimmed milk for 1 h, and then the membranes were incubated with anti-GFP (Abcam, Cambridge, UK) antibodies overnight at 4°C, followed by using peroxidase-linked secondary antibodies (1:10 000) for 1 h in the dark. The bands were detected on an Odyssey infrared imaging system (Odyssey LI-COR Biosciences, Lincoln, NE, USA) according to the manufacturer's instructions. After GFP tag detection, the same membrane was stripped, and then subjected to detect *RUNX2* expression using *RUNX2* antibody (Cell Signaling Technology, Danvers, MA, USA) following the above instructions.

Cell fluorescence

At 48 h after transfection of pEGFP-C1 based wild type and mutant *RUNX2* plasmid, the transfected 293T cells grown on sterile glass coverslips were rinsed with phosphate buffer solution (PBS) three times and fixed in 4% paraformaldehyde for 20 min, and then washed with PBS three times. Thereafter, the nuclei of the cells were stained with 4', 6'-diamidino-2-phenylindole (DAPI; Sigma, St Louis, MO, USA) and the coverslips were mounted on a glass slide. Images were taken with a LSM 5 EXCITER confocal imaging system (Carl Zeiss, Jena, Germany).

Luciferase assay

Before transfection, HEK-293T cells were cultured in six-well plates at a density of 1.5×10^5 /well. At the indicated time, each expression was co-transfected with p6OSE2-luc reporter plasmid, pHRL-TK renilla luciferase vector was also co-transfected and used as an internal control. After 24 h transfection, cell lysates were collected and measured by a Dual-Luciferase Reporter Assay System (Promega, Madison, WI, USA) according to the manufacturer's instructions. All transfection experiments were carried out in triplicate and repeated at least three times. Data were analysed by one-way analysis of variance and $P < 0.05$ was considered statistically significant.

Results

Oral phenotypes in CCD individuals

Seven individuals from four unrelated families with clinical diagnosis of CCD were investigated for the variations in the coding region of *RUNX2* gene. All the participants manifested typical CCD features and three of them were sporadic cases and the others were familial cases (Table 1). Because oral problems are the common complaint of the individuals, we focused on the oral features of those CCD individuals. The oral phenotypes of all participants are displayed as oral panoramic radiograph in Figure 1. Panoramic

Table 1. Clinical and molecular features of CCD individuals

Patient	Family History	Sex (F/M)	Clinical Features of CCD	Mutation				Reference
				Nucleotide ^a	Codon	Type	Location	
Case 1	<i>De novo</i>	F	Classic	577 C>G	R193G	Missense	Runt	This study
Case 2	<i>De novo</i>	M	Classic	774–779 AGTAGG→GA	258fs	Frameshift	PST	This study
Case 3	<i>De novo</i>	M	Classic	1199–1200 ins A	Y400X	Nonsense	PST	This study
Case 4	Familial	F	Classic	674 G>A	R225Q	Missense	Runt	Quack <i>et al.</i> (1)
Case 5	Familial	F	Classic	674G>A	R225Q	Missense	Runt	Quack <i>et al.</i> (1)
Case 6	Familial	F	Classic	674 G>A	R225Q	Missense	Runt	Quack <i>et al.</i> (1)
Case 7	Familial	M	Classic	674 G>A	R225Q	Missense	Runt	Quack <i>et al.</i> (1)

F, female; M, male.

^aNumbering is based on the 521amino acids isoform starting with MASNS.

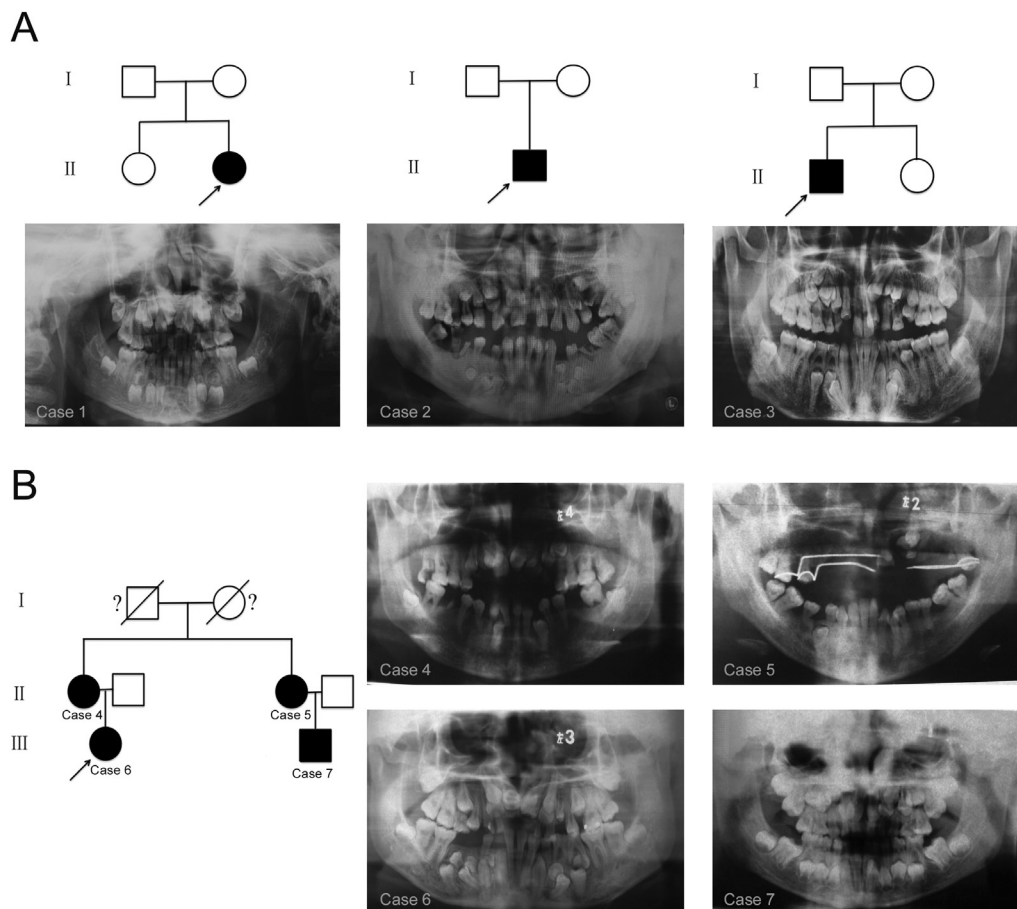


Figure 1. Oral phenotypes of CCD individuals. (A) Pedigree of three unrelated individuals with CCD (arrow indicates the proband) and oral phenotypes of the three novel mutation individuals. (B) Pedigree of familial individuals with CCD and the oral panoramic radiographs.

radiographs show that the individuals with novel *de novo* mutation have supernumerary teeth, retained deciduous teeth and delayed eruption of permanent teeth (Figure 1A). Of the familial cases, case 4 shows supernumerary tooth and delayed eruption of permanent teeth, case 5 shows only supernumerary teeth, while the cases 6 and 7 show supernumerary teeth, retained deciduous teeth and delayed eruption of permanent teeth. The oral phenotypes are summarised in Supplementary Table 1, available at *Mutagenesis* Online. The above phenotype is in line with CCD oral features, which is characterised as supernumerary teeth, retained deciduous teeth and delayed eruption of permanent teeth. Although oral problems are the common complaint of the CCD individuals, the oral phenotypic spectrum in different cases varies strikingly even among familial cases with the same mutations in *RUNX2* gene (Figure 1B).

Mutational analysis

To identify the mutations of *RUNX2* gene in CCD individuals, we amplified the coding region sequence of *RUNX2* gene by PCR and analysed the sequence by the data from NCBI. The results showed that four different types of mutation were identified in seven individuals and these are summarized in Table 1. Of those mutations, three were novel and the other one has been reported previously (1). The three novel mutations were sporadic cases and the reported mutation was a

familial case. As displayed in Figure 2A, case 1 carried a heterozygous 577 C to G mutation in exon 3 of *RUNX2* and located in the Runt domain, resulting in amino acid change of Arg193Gly (p.R193G); case 2 carried a six-nucleotide deletion (AGTAGG) and a two-nucleotide (GA) insertion (774–779 AGTAGG→GA) in exon 5 and seated in PST region, leading to a frameshift from codon 258 to resultant premature stop codon 269; this is the first report of this kind of mutation in CCD marked by deletion and insertion of nucleotide at the same position; case 3 carried a one-nucleotide insertion (c.1199–1200 ins A) in exon 8 and positioned in the PST region, which resulted in a premature stop codon at 400 (p.Y400X). Analysis of familial *RUNX2* from case 1 to 3 revealed no variation, confirming the three mutations as sporadic. The familial mutation was a heterozygous 674 G to A mutation in exon 4 of *RUNX2*, generating amino acid change of Arg225Gln (p.R225Q), it is a typical autosomal dominant mode in this family and no mutation was detected in unaffected members in this family. The conservation analysis results showed that the affected residues in *RUNX2* are highly conserved in different species (Figure 2B), and secondary structure analysis showed that mutation of *RUNX2* gene resulted in the change of structure of *RUNX2* (Figure 3), the changes are mainly located in the Runt domain and have been marked with green arrows. Mutation of the conserved residues and the changes of secondary structure of *RUNX2* appear to impair the function of *RUNX2* protein and cause the CCD.

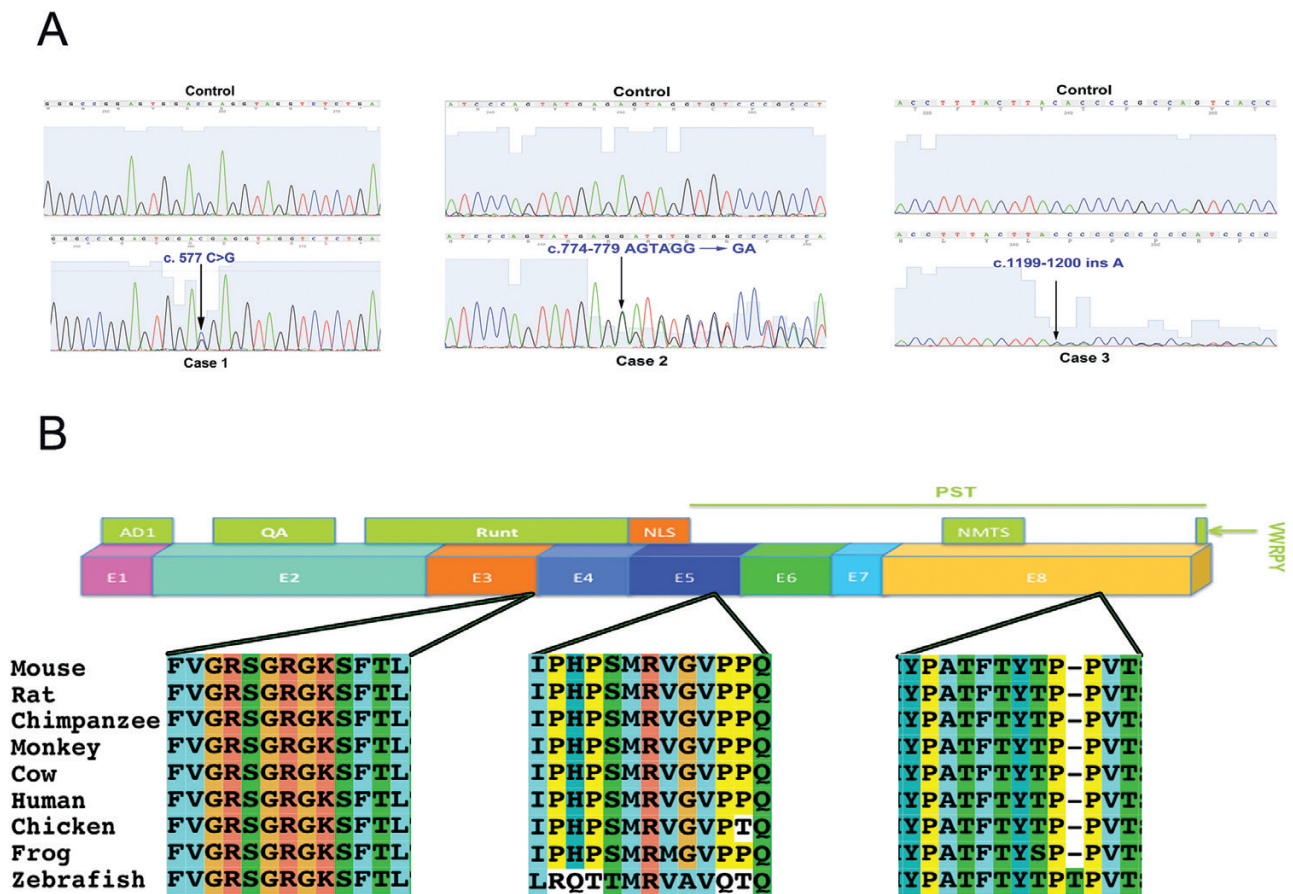


Figure 2. Three novel mutations of *RUNX2* in CCD individuals. (A) Sequence analysis of the three novel mutant *RUNX2*. (B) Diagram of the *RUNX2* protein. AD1-frst activation domain, QA-glutamine-alanine repeats domain, Runt-Runt homologous domain, NLS-nuclear localization signal, PST-proline/serine/threonine rich region, NMTS-nuclear matrix targeting signal, VWRPY-carboxyterminal pentapeptide. Conservation analysis of novel mutations in the probands of case 1 (R193G), case 2 (258fs) and case 3 (Y400X). Affected residues are marked with green arrow in different cases.

Functional analysis of novel RUNX2 mutations

To examine the characteristics of the mutant proteins, 293T cells were transfected with GFP-tagged wild-type or mutated RUNX2 plasmid. Due to the GFP and RUNX2 forming a fusion protein, we detected the GFP and RUNX2 proteins simultaneously, the western blotting results showed that GFP and RUNX2 proteins were at the bands, which means that the fusion protein expressed properly (Figure 4A). Western blotting results revealed that wild-type RUNX2 generated 83 kDa functional GFP-RUNX2 fusion protein, while 258fs and Y400X mutant RUNX2 proteins produced 55 kDa and 69 kDa non-functional truncated proteins due to premature stop codon. Missense

mutation at c.577 C>G has no influence on the length of RUNX2 protein (Figure 4A). As seen in Figure 4A, the mutant RUNX2 in case 2 was undetected by RUNX2 antibody because the 258fs mutation produced a premature stop codon at 269, while this antibody was designed to correspond to residues surrounding Ala273 of RUNX2.

The RUNX2 protein has an NLS next to the C-terminal of Runt domain; this sequence is essential for the nucleus of RUNX2 protein. To explore whether the three novel mutations could affect the subcellular distribution of RUNX2, we transfected HEK-293T cells with GFP-tagged wild-type or mutants RUNX2 plasmids. Cell fluorescence results showed that the signal of GFP control was evenly



Figure 3. Secondary structure analysis of mutated RUNX2. Pink cylinders are represents the helix, yellow arrows presents the strand, and the straight line represents the coil. Transformations have been marked with green arrows.

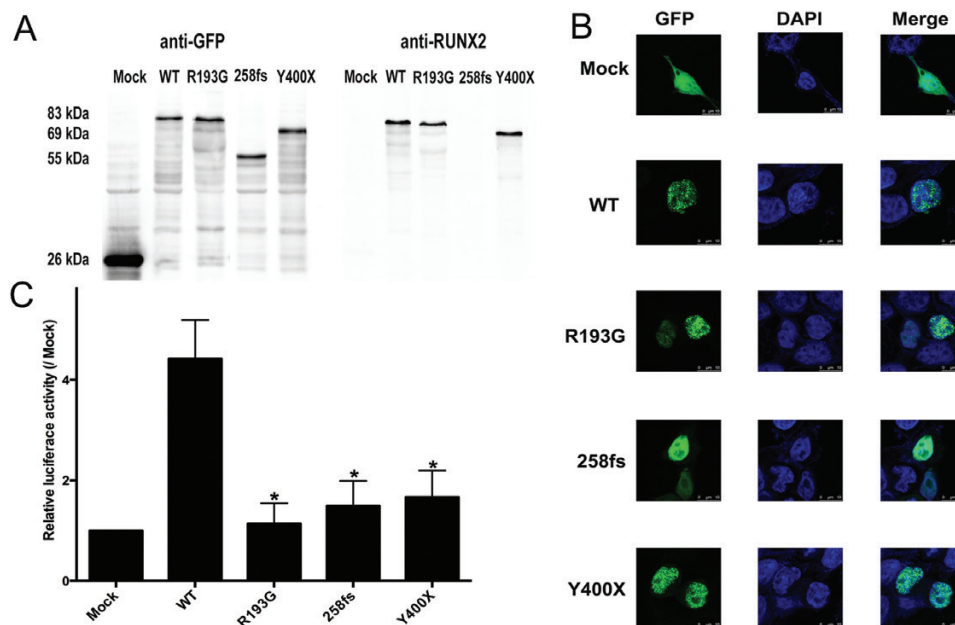


Figure 4. Functional analysis of novel *RUNX2* mutants. (A) Western blotting analysis of GFP-*RUNX2* fusion proteins after 48 h transfection of 293T cells. The anti-GFP and anti-*RUNX2* antibodies were used to perform western blotting. 258fs and Y400X mutations caused non-functional truncated *RUNX2* proteins. (B) Subcellular localisation of mutant *RUNX2*-GFP fusion protein in 293T cells. (C) Luciferase assay to evaluate the role of *RUNX2* proteins in the transactivation of the osteocalcin promoter. * $P < 0.05$ versus WT-transfected cells.

distributed throughout the cytoplasm and nucleus, while the wild-type and the three novel mutant *RUNX2* proteins were localised exclusively in the nucleus, indicating that the ability to accumulate in the nucleus is not impaired by those novel mutations (Figure 4B). Thus, mutations outside the NLS had no influence on the function of the NLS in accumulating *RUNX2* in nucleus.

Since the novel mutations are located in the Runt domain or PST region, those regions are necessary for the transcriptional regulation. Thus, although the novel mutant *RUNX2* proteins can accumulate in the nucleus, we still wondered whether the novel mutations had influence on the transactivation activity. To verify the effects of the three *RUNX2* mutants on the transactivation activity, we performed a dual-luciferase reporter assay as described above to examine whether the mutant *RUNX2* proteins could trans-activate the downstream specific target promoter, p6OSE2-luc. Luciferase activity results showed that the three novel mutants significantly reduced the transcriptional activity of the downstream target gene compared to the wild-type *RUNX2* protein (Figure 4C).

Discussion

RUNX2 is a vital transcription factor in regulating the skeletal development and bone formation. Studies have revealed that *RUNX2* mutation is responsible for autosomal dominant skeletal disorder CCD (4,5). We described four different mutations in *RUNX2* gene in seven CCD individuals in this study. Of these mutations, three were novel and the other one had previously been reported (1). Functional analysis of novel mutant *RUNX2* was undertaken to explore the characteristics of the novel mutations of *RUNX2*.

In this study, all the individuals showed classic CCD features, including hypoplastic clavicles, open fontanelle and dental abnormalities. The clinical features showed a wide difference between those individuals, even among familial cases. The diversity clinical features of our CCD individuals are consistent with results from previous

studies (5). Lou *et al.* (19) generated a homozygous *RUNX2*^{neo7/neo7} mice model and proved that less than 70% of wild-type *RUNX2* level resulted in CCD phenotype whereas higher level of *RUNX2* showed no skeletal abnormalities. The three novel mutations were found in different regions of *RUNX2*; those three novel mutations may result in different expression efficiency of *RUNX2* and in skeletal phenotypic variability in CCD individuals. Supernumerary teeth are very common in CCD, yet supernumerary teeth number has a striking variability in CCD individuals. Togo *et al.* (20) revealed that USAG-1 and *RUNX2* act in an antagonistic manner during supernumerary teeth formation; the three novel mutations of *RUNX2* may lead to different crosstalk mode between USAG-1 and *RUNX2* and generated the striking variations in supernumerary teeth.

Runt domain is a highly conserved DNA-binding domain, which guides the *RUNX2* protein binds to a consensus DNA sequence. The Runt domain also interacts closely with the CBF β , though CBF β does not contact with DNA directly, it enhances DNA binding by the *RUNX2* protein upon heterodimerisation (21). Missense mutation R193G was located in Runt domain and the conservation analysis showed the affected residues are highly conserved in different species, indicating the R193G mutation may impair the binding ability of *RUNX2*. The structure and function of protein are closely related; the transformation of protein structure can influence the function of protein (22,23). The secondary structure analysis of R193G, 258fs and Y400X results revealed that the three novel mutants altered the Runt domain secondary structure of *RUNX2* proteins. Interestingly, though the 258fs and Y400X mutations were positioned in PST region, they can convert the secondary structure of Runt domain areas. Summarily, the secondary structure transformation of R193G, 258fs and Y400X may lead to the defect of heterodimerisation activity and possibly impair the function of *RUNX2* proteins.

258fs mutation caused a frameshift from codon 258 to the premature stop codon 269, leading to a truncated *RUNX2* protein at a length of 268 amino acids. Y400X mutation is a nonsense mutation, and

formed a premature stop codon at 400, leading to a RUNX2 protein truncated at a length of 399 amino acids. Previous studies demonstrate that truncated protein may degrade rapidly (24,25). To understand the stability of the novel mutated RUNX2 proteins, we performed western blotting. As shown in Figure 4A, we found that 258fs and Y400X mutations caused non-functional truncated proteins and no-degraded truncated RUNX2 proteins produced. NLS is composed of nine amino acids and located at the C-terminal end of the Runt domain, and NLS is essential for the nuclear localisation of RUNX2 protein (1). The three novel mutations did not destroy the integrity of NLS, so the three novel RUNX2 mutant proteins can accumulate in the nucleus and the results of nuclear localisation are in line with the previous research results (26). Though the three novel mutations did not affect the nuclear localisation of RUNX2 proteins, it may damage the transcriptional activity of RUNX2. To test this hypothesis, we took a reporter assay and the results demonstrated that the three novel mutants significantly reduced the transcriptional activity on the downstream target gene. Therefore, although the three novel mutants did not influence nuclear localisation, they failed to activate the promoter of osteocalcin and severely impaired the transcriptional activity of RUNX2, and produced non-functional truncated RUNX2 proteins in individuals with 258fs and Y400X mutations. Taken together, the functional analysis of the mutant RUNX2 proteins results demonstrate that the loss of function of RUNX2 is responsible for CCD.

Our results firstly described three novel mutations (R193G, 258fs, Y400X) and broaden the spectrum of RUNX2 mutations in CCD individuals. Conservation, structure prediction and functional analysis of mutant RUNX2 proteins revealed that the three novel RUNX2 mutations impaired the function of RUNX2 and resulted in the CCD phenotype. Further studies are required to explore the molecular regulatory mechanism of the mutant proteins.

Supplementary data

Supplementary Table 1 is available at *Mutagenesis* Online.

Funding

This work was supported by the National Natural Science Foundation of China (81570961 and 81172556) and Beijing Natural Science Foundation (7172240).

Acknowledgements

We are grateful to the CCD individuals for participating in this study.

Conflict of interest statement: None declared.

References

- Quack, I., Vonderstrass, B., Stock, M., *et al.* (1999) Mutation analysis of core binding factor A1 in patients with cleidocranial dysplasia. *Am. J. Hum. Genet.*, 65, 1268–1278.
- Lukinmaa, P. L., Jensen, B. L., Thesleff, I., Andreasen, J. O. and Kreiborg, S. (1995) Histological observations of teeth and periodontal tissues in cleidocranial dysplasia imply increased activity of odontogenic epithelium and abnormal bone remodeling. *J. Craniofac. Genet. Dev. Biol.*, 15, 212–221.
- Chang, H., Wei, J., Wang, Y., Jia, J., Gao, X., Li, X. and Feng, H. (2015) Restorative treatment strategies for patients with cleidocranial dysplasia. *Acta Odontol. Scand.*, 73, 447–453.
- Lee, B., Thirunavukkarasu, K., Zhou, L., Pastore, L., Baldini, A., Hecht, J., Geoffroy, V., Ducy, P. and Karsenty, G. (1997) Missense mutations abolishing DNA binding of the osteoblast-specific transcription factor OSF2/CBFA1 in cleidocranial dysplasia. *Nat. Genet.*, 16, 307–310.
- Mundlos, S. (1999) Cleidocranial dysplasia: clinical and molecular genetics. *J. Med. Genet.*, 36, 177–182.
- Komori, T., Yagi, H., Nomura, S., *et al.* (1997) Targeted disruption of Cbfa1 results in a complete lack of bone formation owing to maturational arrest of osteoblasts. *Cell*, 89, 755–764.
- Otto, F., Thornell, A. P., Crompton, T., *et al.* (1997) Cbfa1, a candidate gene for cleidocranial dysplasia syndrome, is essential for osteoblast differentiation and bone development. *Cell*, 89, 765–771.
- Ducy, P., Zhang, R., Geoffroy, V., Ridall, A. L. and Karsenty, G. (1997) Osf2/Cbfa1: a transcriptional activator of osteoblast differentiation. *Cell*, 89, 747–754.
- Javed, A., Barnes, G. L., Jasanya, B. O., Stein, J. L., Gerstenfeld, L., Lian, J. B. and Stein, G. S. (2001) runt homology domain transcription factors (Runx, Cbfa, and AML) mediate repression of the bone sialoprotein promoter: evidence for promoter context-dependent activity of Cbfa proteins. *Mol. Cell. Biol.*, 21, 2891–2905.
- Sato, M., Morii, E., Komori, T., *et al.* (1998) Transcriptional regulation of osteopontin gene in vivo by PEBP2alphaA/CBFA1 and ETS1 in the skeletal tissues. *Oncogene*, 17, 1517–1525.
- Liu, T. M. and Lee, E. H. (2013) Transcriptional regulatory cascades in Runx2-dependent bone development. *Tissue Eng. Part B. Rev.*, 19, 254–263.
- Hecht, J., Seitz, V., Urban, M., *et al.* (2007) Detection of novel skeletogenesis target genes by comprehensive analysis of a Runx2(-/-) mouse model. *Gene Expr. Patterns*, 7, 102–112.
- Chung, C. R., Tsuji, K., Nifuji, A., Komori, T., Soma, K. and Noda, M. (2004) Micro-CT evaluation of tooth, calvaria and mechanical stress-induced tooth movement in adult Runx2/Cbfa1 heterozygous knock-out mice. *J. Med. Dent. Sci.*, 51, 105–113.
- Zou, S. J., D'Souza, R. N., Ahlberg, T. and Bronckers, A. L. (2003) Tooth eruption and cementum formation in the Runx2/Cbfa1 heterozygous mouse. *Arch. Oral Biol.*, 48, 673–677.
- Xiao, Z. S., Hjelmeland, A. B. and Quarles, L. D. (2004) Selective deficiency of the “bone-related” Runx2-II unexpectedly preserves osteoblast-mediated skeletogenesis. *J. Biol. Chem.*, 279, 20307–20313.
- Zaidi, S. K., Javed, A., Choi, J. Y., van Wijnen, A. J., Stein, J. L., Lian, J. B. and Stein, G. S. (2001) A specific targeting signal directs Runx2/Cbfa1 to subnuclear domains and contributes to transactivation of the osteocalcin gene. *J. Cell Sci.*, 114, 3093–3102.
- Singh, A., Goswami, M., Pradhan, G., Han, M. S., Choi, J. Y. and Kapoor, S. (2015) Cleidocranial dysplasia with normal clavicles: a report of a novel genotype and a review of seven previous cases. *Mol. Syndromol.*, 6, 83–86.
- Hedegaard, C., Bendixen, E., Jensen, P. H., Bendixen, C. and Larsen, K. (2009) An exonic insertion encodes an alanine stretch in porcine synapsin I. *Biochem. Genet.*, 47, 812–816.
- Lou, Y., Javed, A., Hussain, S., *et al.* (2009) A Runx2 threshold for the cleidocranial dysplasia phenotype. *Hum. Mol. Genet.*, 18, 556–568.
- Togo, Y., Takahashi, K., Saito, K., *et al.* (2016) Antagonistic functions of USAG-1 and RUNX2 during tooth development. *PLoS One*, 11, e0161067.
- Tahirov, T. H., Inoue-Bungo, T., Morii, H., *et al.* (2001) Structural analyses of DNA recognition by the AML1/Runx-1 Runt domain and its allosteric control by CBFbeta. *Cell*, 104, 755–767.
- Monteiro, P. and Feng, G. (2017) SHANK proteins: roles at the synapse and in autism spectrum disorder. *Nat. Rev. Neurosci.*, 18, 147–157.
- Wong, S. W., Liu, H. C., Han, D., Chang, H. G., Zhao, H. S., Wang, Y. X. and Feng, H. L. (2014) A novel non-stop mutation in MSX1 causing autosomal dominant non-syndromic oligodontia. *Mutagenesis*, 29, 319–323.
- Hashimoto, S., Tsukada, S., Matsushita, M., *et al.* (1996) Identification of Bruton's tyrosine kinase (Btk) gene mutations and characterization of the derived proteins in 35 X-linked agammaglobulinemia families: a nationwide study of Btk deficiency in Japan. *Blood*, 88, 561–573.
- Akeson, A. L., Wiginton, D. A. and Hutton, J. J. (1989) Normal and mutant human adenosine deaminase genes. *J. Cell. Biochem.*, 39, 217–228.
- Zhang, C., Zheng, S., Wang, Y., Zhao, Y., Zhu, J. and Ge, L. (2010) Mutational analysis of RUNX2 gene in Chinese patients with cleidocranial dysplasia. *Mutagenesis*, 25, 589–594.